Order-disorder and electronic transitions in $Ag_{2+\delta}S$ single crystals studied by photoemission spectroscopy

S. R. Barman, N. Shanthi, A. K. Shukla, and D. D. Sarma*
Solid State and Structural Chemistry Unit, Indian Institute of Science, Bangalore 560 012, India
(Received 17 May 1995; revised manuscript received 25 September 1995)

The electronic structure of $Ag_{2+\delta}S$ single crystals is investigated as a function of temperature and nonstoichiometry, δ. It is shown that the stoichiometric, low-temperature α-Ag_2S phase is a band insulator with correlation effects further increasing the band gap. The results suggest that the metal-insulator transition observed with increase in δ from the stoichiometric ($\delta=0$) phase in the high-temperature β-$Ag_{2+\delta}S$ is due to the tuning of the Fermi energy through the mobility edge. The increase in conductivity associated with the insulator-to-insulator transition across the α-β phase transformation in the stoichiometric Ag_2S is suggested to arise from the order-disorder transition and the consequent redistribution of states near the top of the valence band.

I. INTRODUCTION

Silver sulfide exhibits an order-disorder transition at 450 K. The high-temperature disordered phase has a high Ag^+-ion conductivity just as in the high-temperature α phase of AgI. This order-disorder transition has often been described in terms of melting of the silver sublattice. In the high-temperature superionic β-Ag_2S phase, the S sublattice is ordered in a body-centered-cubic (bcc) lattice, while the four Ag ions in the unit cell were reported[1] to be distributed among the octahedrally coordinated 6(b), tetrahedrally coordinated 12(d), and triangularly coordinated 24(h) positions of the $Im3m$ space group. However, a more recent neutron-diffraction study[2] has shown that the Ag ions occupy only the tetrahedral and octahedral sites with an occupancy ratio of about 3:1 just above the transition temperature $T_{\alpha\beta}$ (=450 K). At higher temperatures the tetrahedral occupancy increases at the expense of the octahedral occupancy, and above 533 K the occupied sites are solely tetrahedral. With the help of coulometrically controlled measurements, it has been shown[3] that the β-Ag_2S phase can accommodate excess silver and thus compositions of $Ag_{2+\delta}S$ with $0.0 \leqslant \delta \leqslant 2.5\times10^{-3}$ have been prepared and studied. By contrast, α-Ag_2S has a monoclinic structure with space group $P2_1/c$ space group.[4] There are two types of Ag ions of equal number in the unit cell which occupy positions close to the ideal [2+4] octahedral and tetrahedral coordinations of the distorted body-centered cubic array. We show the arrangements of various atoms in the low-temperature α-Ag_2S phase in Fig. 1(a), illustrating the distorted octahedral and tetrahedral coordinations of Ag^+ ions. In Fig. 1(b) we schematically show the octahedral and tetrahedral sites available for the Ag^+-ion occupancy in the high-temperature undistorted body-centered cubic structure of β-Ag_2S.

Across $T_{\alpha\beta}$, Ag^+-ion conductivity increases by about two orders of magnitude.[6] While α-Ag_2S is electronically insulating, the electronic conductivity in the β-$Ag_{2+\delta}S$ phase increases by three orders of magnitude across the order-disorder transition and could vary 100–1000 $\Omega^{-1}\,cm^{-1}$ depending on the value of δ.[5,7] This jump in conductivity has been ascribed[5] to the crystallographic disorder brought about by melting of the cation sublattice in β-Ag_2S. *In situ* conductivity measurements on coulometrically controlled β-$Ag_{2+\delta}S$ samples show an insulating behavior for $\delta \leqslant 5\times10^{-4}$ and metallic nature for samples with

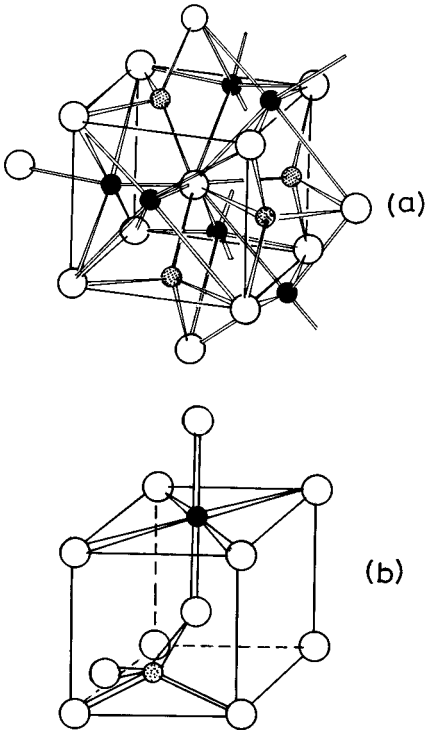

FIG. 1. (a) Atomic arrangements in the distorted body-centered-cubic structure of low-temperature α-Ag_2S (adopted from Ref. 2) showing the S (open circles), octahedrally coordinated Ag (filled circles), and tetrahedrally coordinated Ag (shaded circles). (b) Atomic arrangements of S ions (open circles) in the body-centered cubic structure of the high-temperature β-Ag_2S phase. The filled circle shows a typical octahedral and the shaded circle shows a typical tetrahedral site.

$\delta > 5\times10^{-4}$.[7,8] This insulator-to-metal transition in β-$Ag_{2+\delta}S$ arising from a delicate control of δ in the regime of small δ has been suggested[8] to be due to the excess charge-carrier doping. Resistivity and thermopower studies[5,7] suggest that this transition is driven by disorder effects attributed to Anderson localization.[9]

An earlier x-ray photoemission (XP) and Auger electron (AE) spectroscopic study[10] on polycrystalline β-$Ag_{2+\delta}S$ found changes in the valence band XP spectra which reflected the conductivity behavior of these samples. The $K\beta$ emission and K absorption spectra[11] of S in α-Ag_2S show the existence of the insulating gap and suggest that the bottom of the conduction band arises mainly from S $4p$-like states. In this study, we report the electronic structures of α- and β-Ag_2S using x-ray photoemission, ultraviolet photoemission (UP), and bremsstrahlung isochromat (BI) spectroscopies in conjunction with various *ab initio* band structure results in order to investigate effects of disorder in the Ag sublattice across the α-β transition as well as the origin of the insulator-to-metal transition driven by the silver nonstoichiometry δ in the β-$Ag_{2+\delta}S$ phase.

II. EXPERIMENT

Single crystals of $Ag_{2+\delta}S$ were prepared using the chemical-vapor-transport method and the extent of silver nonstoichiometry δ was controlled by coulometric measurements as described in Ref. 12. In brief, the method used earlier[7,8] to make $Ag_{2+\delta}S$ crystals was modified to grow larger samples suitable for electron spectroscopy. Samples with $\delta=0$ (referred to in the text henceforth as Ag_2S) and $\delta=2\times10^{-3}$ (referred to as $Ag_{2+\delta}S$) were prepared coulometrically by using the atomic galvanic cell: $Ag|\alpha\text{-}AgI|Ag_{2+\delta}S|Pt$. Using the left-hand side of the galvanic cell as the anode and imposing an anodic current i, Ag^+ ions are made to flow through the silver sulfide sample via silver iodide, which is a purely ionic conductor; simultaneously electrons flow through the Pt lead in the right-hand side of the cell into the silver sulfide leading to an increase of Ag in the specimen. The degree of nonstoichiometry, δ, of the $Ag_{2+\delta}S$ samples in the β phase can also be reduced by reversing the situation and applying a cathodic current. The exact value of δ was determined by the Faraday Laws: $\delta = \int_0^t i/n_s F dt$, where i is the current passed through the galvanic cell over a time t, n_s is the number of moles of S in Ag_2S, and F is the Faraday constant. Since the current flowing through and the total duration can be measured with great accuracies, δ can be determined in this method easily to an accuracy of 10^{-4}. More details of coulometric techniques can be found in Refs. 3, 7, and 8. The monocrystalline nature of the samples were confirmed by Laue x-ray diffraction photographs. Conductivity measurements showed the expected behavior in both the samples and the values of band gaps for the stoichiometric α- and β-Ag_2S were estimated to be 1.2 and 0.4 eV, respectively, in agreement with the literature.[5,7,13]

Clean surfaces were obtained for photoemission experiments by *in situ* mechanical scraping of the sample surface with an alumina file inside the ultra-high-vacuum chamber of the spectrometer. The surface cleanliness was monitored by recording O 1s and C 1s core-level spectral regions, both of which were below the detection level. The surface showed high stability against contamination. The spectra for both Ag_2S and $Ag_{2+\delta}S$ samples were measured at various temperatures above and below $T_{\alpha\beta}$. Here, we report the spectra recorded at 400 ± 10 K and 600 ± 10 K for Ag_2S, and at 600 ± 10 K for $Ag_{2+\delta}S$.

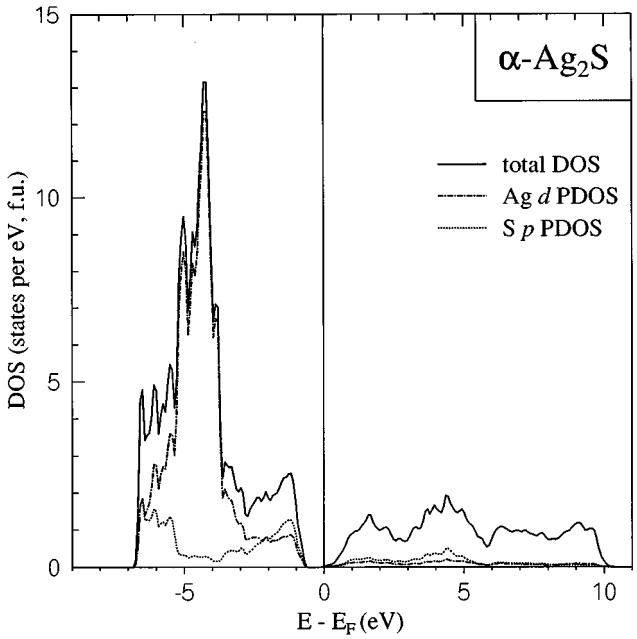

FIG. 2. The total DOS, and Ag d and S p PDOS for α-Ag_2S calculated within LMTO-ASA.

Self-consistent linearized muffin-tin-orbital calculations within the atomic-sphere approximation (LMTO-ASA) were performed for stoichiometric Ag_2S in the monoclinic structure with four formula units (f.u.) per unit cell and lattice parameters: $a=4.231$ Å, $b=6.930$ Å, $c=9.526$ Å, and $\beta=125.48°$.[4] No empty sphere was required in these calculations in order to satisfy the volume-filling criterion with reasonable overlaps. The convergence was carried out with 504 k points in the irreducible part of the Brillouin zone. The energy E_ν^l for each angular momentum partial wave was chosen to be at the center of gravity of the occupied parts of the corresponding partial density of states (PDOS). But to calculate the unoccupied part of the DOS accurately, values of E_ν^l were shifted to 6 eV above E_F for all states except for Ag d and S s states. Matrix elements corresponding to XP and BI processes were calculated following the method of Winter *et al.*[14] and included in constructing the corresponding calculated spectra from various PDOS along with resolution and lifetime broadenings.[15] The calculated results for the occupied states had to be rigidly shifted by about 1.5 eV towards higher binding energy while comparing with the experimental data. This is because the band gap tends to be underestimated in such band structure calculations within the local density approximation.

III. RESULTS AND DISCUSSION

Figure 2 shows the total density of states and Ag d and S p PDOS of α-Ag_2S calculated within LMTO-ASA. While the occupied part of the DOS is almost completely domi-

nated by these two partial DOS, the unoccupied part has substantial contributions from other partial DOS, such as Ag s and p and S s states which are not shown in the figure for the sake of clarity. However, contributions of these states to the unoccupied (BI) spectra will be discussed later in the text (also see Fig. 4). The E_F has been placed at the bottom of the conduction band, as observed in the experiment. The DOS shows a clear gap of about 0.7 eV for this insulating system which is somewhat smaller than the value (1.2 eV) obtained from resistivity studies. This is a well known drawback of any calculation based on the local density approximation which tends to underestimate band gaps.[16] However, the correct prediction of an insulating state from the band structure calculation confirms that the origin of this conductivity gap lies primarily in one-electron effects; substantial correlation effects due to the presence of large intraatomic Coulomb interaction (U_{dd}) within the Ag d states increases the magnitude of the gap. The occupied DOS below E_F is mostly dominated by Ag d PDOS which peaks at -4.3 eV. The Ag d PDOS is nearly constant between -2.8 and -1 eV. The dominant contribution to the DOS in this energy range, however, comes from the S p PDOS, which also has a substantial contribution between -6.7 and -5.3 eV and a small contribution between -5.3 and -2.8 eV. The description of the bonding and the electronic structure described here is similar to other compounds involving the transition metal d and partner p interactions, such as silicides and aluminides of transition elements.[17] In all these cases, we find bonding d-p states appearing at the lowest-energy region (between -5 and -7 eV in Fig. 2). The bonding region is followed by a region where the transition metal d states dominate (between about -3 and -5 eV in Fig. 2); this is the so-called nonbonding states.[17] The highest-energy states arise from the antibonding interaction between the transition metal d and the ligand p states; this is the energy region between about -3 and -0.5 eV in Fig. 2. It is to be noted that all these three regions (bonding, nonbonding, and antibonding) are occupied in the case of Ag_2S owing to the Ag $4d^{10}$ and S $3p^6$ electronic configurations; consequently all these states appear below E_F in Fig. 2. Thus, the unoccupied part of the DOS within the first 10 eV above E_F arises primarily from Ag $5s$ and $5p$ and S $4s$, $4p$ and $3d$ like continuum states. These states, being very extended in nature, give rise to a rather wide band DOS. The Ag d partial DOS contribute in these unoccupied parts via hybridization with these extended states, exhibiting two broad structures at about 1.6 and 4.4 eV above E_F; the Ag d contribution in the unoccupied part is considerably smaller than that in the occupied part.

In Fig. 3, we show the XP spectrum of α-Ag_2S recorded at 400 K with Al $K\alpha$ radiation. The spectrum indicates the existence of the gap which is observed more clearly in the He I UP spectrum with better resolution (inset to Fig. 3). The estimate of the gap is about 1 ± 0.1 eV from the UP spectrum. The XP spectrum exhibits a step around -1.8 eV and a peak at -5.2 eV with a shoulder at -6 eV. The calculated XP spectrum with the Ag d and S p components is also shown in Fig. 3. The agreement between the calculated and the experimental spectra is satisfactory. However, the shoulder at -6 eV in the experimental spectrum is not reproduced in the calculation. This is most probably due to the neglect of spin-orbit interaction in the present calculation. An interesting aspect to be noted in the calculation is that the XP spectrum at this photon energy is dominated entirely by Ag d-like states, the contribution from S p-like states being almost negligible in comparison. We could not calculate the UP spectrum since the approximations involved in the calculation of the XP spectrum are not valid in the low-photon-energy range.[14] However, we have compared the UP spectrum with the calculated DOS and PDOS (from Fig. 2) in the inset to Fig. 3. Though the comparison of the exact spectral shapes is not meaningful due to the neglect of transition matrix elements, different features in the experimental spectrum can be associated with the calculated DOS. The UP spectrum exhibits a step around -1.8 eV and peaks at -5.3 eV with a shoulder at -6.1 eV in close similarity to the features observed in the XP spectrum. However, the UP spectrum exhibits an extra feature at -3.8 eV which is not clearly seen in the XP spectrum, probably due to poorer resolution in the latter. A close inspection of the XP spectrum in the same energy range, however, suggests that it is also present there with comparable intensity. Thus, we believe that this feature at -3.8 eV is not a surface related state and this is further evidenced by an exposure of the sample to oxygen ($\sim$5 L) which does not alter this spectral feature. More specifically, the feature at -3.8 eV in the UP spectrum seems to have a counterpart in the calculated DOS. This feature may arise from a sizable interaction of the Ag d and S p states as evidenced by the simultaneous presence of these states in this energy range. However, further studies on oriented surfaces using angle-resolved photoemission technique will yield more information on the nature of these states.

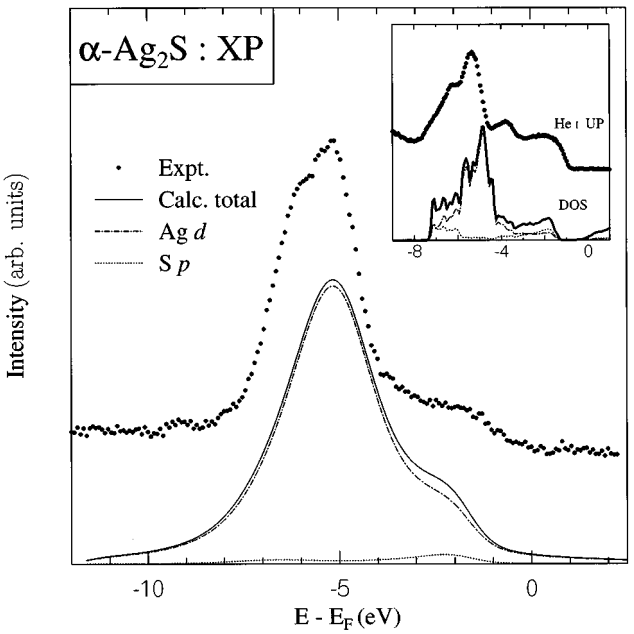

FIG. 3. The experimental XP spectrum (dots) for α-Ag_2S and the calculated XP spectrum, with Ag d and S p components. The inset shows the experimental UP spectrum (dots) for α-Ag_2S and the total DOS, and Ag d and S p PDOS from Fig. 1. In both the main figure and the inset the calculated was shifted by 1.5 eV towards higher binding energy (see text).

The experimental BI spectrum recorded at 400 K as well as the calculated BI spectrum for α-Ag_2S are shown in Fig. 4. The experimental spectrum exhibits two prominent fea-

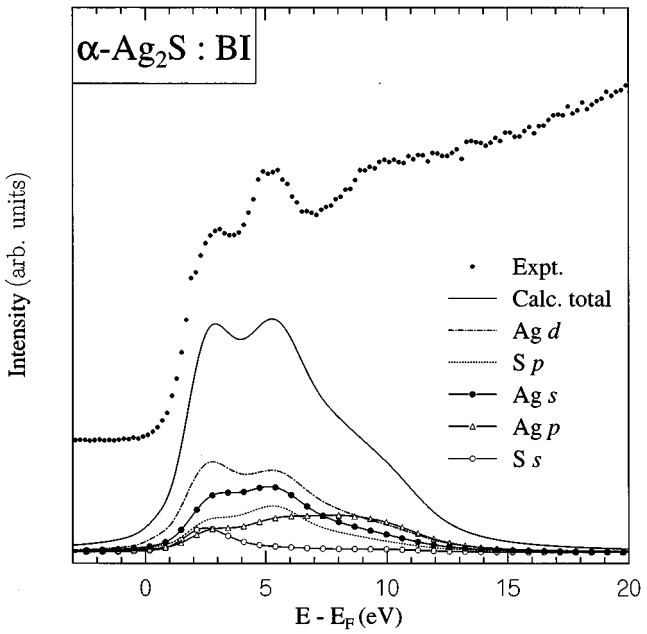

FIG. 4. The experimental BI spectrum (dots) for α-Ag_2S. The calculated BI spectrum along with the Ag d, S p, Ag s, Ag p, and S s components is shown for comparison.

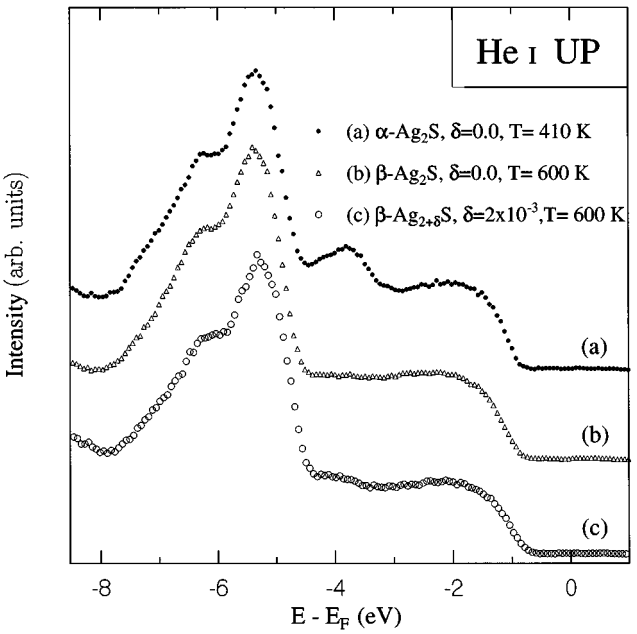

FIG. 5. He I UP spectra of (a) α-Ag_2S at 400 K, (b) β-Ag_2S, and (c) β-$Ag_{2+\delta}S$ with $\delta=2\times10^{-3}$ at 600 K.

tures at 3 and 5.2 eV, and a broad and weak feature at about 9.6 eV. The calculated BI spectrum agrees well with experiment up to about 10 eV. In contrast to the calculation, the experimental spectrum continues to increase beyond this energy due to the presence of high lying continuum states and an inelastic scattering background which are not included in the calculation. The different site and angular momentum projected components for the calculated BI spectrum indicate that the most dominant contribution in the 0–10 eV energy range is due to Ag d-like states. This may appear unusual since Ag in Ag_2S is in a formal 1+ valence state with d^{10} electron configuration and consequently has no unoccupied d state. Band structure results shown in Fig. 2 partly justify this expectation as there appears to be only minor contributions from Ag d states in the unoccupied part of the DOS. However, a very large transition probability for the Ag d states relative to that of any other state makes the Ag d-contribution to be dominant in the spectrum of the unoccupied part of the DOS. The next major contribution to the spectral features at 3 and 5.2 eV arises from Ag s-like states followed by S p- and Ag p-like states. The S s-like states have small contribution only to the feature at 3.0 eV while the predominant contribution to the feature at 9.6 eV arises from Ag p- and Ag d-like states.

Having discussed the electronic structure of stoichiometric and ordered α-Ag_2S, we now focus on the question relating to the effect of disorder and nonstoichiometry. We have recorded the He I UP spectra of β-Ag_2S ($\delta=0$) and that of β-$Ag_{2+\delta}S$ ($\delta=2\times10^{-3}$) at 600 K. These spectra are shown in Fig. 5b,c along with the spectrum for α-Ag_2S at 400 K [Fig. 5(a)]. A comparison of UP spectra of α-Ag_2S at 400 K and β-Ag_2S at 600 K [Figs. 5(a,b)] provides the direct description of spectral modifications across the order-disorder transition at $T_{\alpha\beta}$. We find that the only difference in the high-temperature spectrum is the absence of the -3.8 eV feature, while the rest of the two spectra are almost identical. Thus, the absence of long-range order in the Ag sublattice does not modify the Ag d-related features between -4.5 and -7.5 eV. This suggests that this part of the spectrum is dominated by local interactions. It is to be noted that α-Ag_2S has two 2.49 Å and four 3.43 Å Ag-S bond distances for the octahedral sites and 2.52 Å, 2.6 Å, 2.7 Å, and 2.99 Å for the tetrahedral sites.[2] Thus there are rather short Ag-S bonds (2.49 Å for the octahedral and 2.52 and 2.6 Å for the tetrahedral sites) arising from the distorted body-centered-cubic array of the S ions. These short bonds are expected to give rise to strong Ag d-S p interactions. In the high temperature β-Ag_2S phase, the S ions form a regular body-centered-cubic array; in this structure the equilibrium separations for the regular octahedral and tetrahedral sites are 3.44 and 2.72 Å, respectively. Thus, the Ag-S interactions is expected to be considerably weakened due to the absence of any short Ag-S bonds in the high-temperature phase. Thus, the absence of the -3.8 eV feature in the β-Ag_2S spectrum is possibly due to this disruption of the Ag-S bonds.

Within the limits of the instrumental resolution and sensitivity, we do not observe any clear effect of disorder induced by silver-sublattice melting on any other spectral region, particularly the near E_F region, which can account for the jump in conductivity at $T_{\alpha\beta}$. The UP spectrum for β-$Ag_{2+\delta}S$ at 600 K [Fig. 5(c)] is also very similar to that for β-Ag_2S at the same temperature exhibiting no detectable DOS in the near E_F region. This is not surprising because such a small concentration of excess Ag (corresponding to $\delta=2\times10^{-3}$) and the consequent movement of E_F are well below the detection limit of the experimental technique employed here. Also, the photoemission cross section corresponding to the DOS in the near E_F region, due to the disorder induced band broadening or structural changes at $T_{\alpha\beta}$, is possibly low and thus not detected in the photoemission experiments.

The fact that we do not see any difference between the insulating and the metallic samples with different δ values above $T_{\alpha\beta}$ clearly establishes that there is no large shift of E_F between these two compositions. Various peak positions in UP and BI spectra of α-Ag_2S and β-Ag_2S are also very similar. This indicates that in every case E_F is pinned to the bottom of the conduction band which can arise from a very small amount of sulphur vacancy even in α-Ag_2S. The states pinning E_F are probably localized due to Anderson localization[9] and are of too low an intensity to be observed by photoemission techniques. Above $T_{\alpha\beta}$, the excess silver in β-$Ag_{2+\delta}S$ dissolves into the matrix donating electrons into the system. This moves E_F into the conduction band beyond the mobility edge[18] making the system metallic. However, it is to be noted that the movement of E_F is small as the extent of the increase in electron concentration with $\delta=2\times10^{-3}$ compared to the case of $\delta=0$, is quite small and consequently is not detected in the spectroscopic measurements. In the case of β-Ag_2S, E_F remains below the mobility edge as no excess silver is present to donate electrons. Thus, the present spectroscopic results, indicating no detectable change in the peak positions, are consistent with the suggestion[5,7] that Anderson localization is responsible for the insulating state in β-Ag_2S sample near $\delta\approx0$ and the metal-insulator transition with increase in δ value arises from the tuning of E_F through the mobility edge. The present results, however, do not support the concept of a large movement of E_F at the metal-insulator transition.[8]

While the metal-insulator transition in the high-temperature β phase is understandable in terms of the above discussion, the nature of the insulator-to-insulator transition across $T_{\alpha\beta}$ in Ag_2S accompanied by a three-orders-of-magnitude change in resistivity for $\delta\approx0$ has not been discussed in the literature. It is also to be noted that resistivity measurements indicate that in the stoichiometric Ag_2S sample the band gap changes from about 1.2 to 0.4 eV on heating the sample through $T_{\alpha\beta}$. While the UP spectrum of the low-temperature α phase shown in Fig. 5(a) exhibits a gap ($\sim$1 eV) in agreement with the resistivity data, the spectrum corresponding to the high-temperature β-Ag_2S phase [Fig. 5(b)] does not show any reduction in the band gap, unlike the transport measurements. This can only happen if the reduction in the band gap in the β phase involves very low DOS below the level of detection of the present technique. We can make a rough estimate of the relevant DOS in this case from the transport measurements. It is easy to calculate the order of magnitude increase in conductivity at 450 K when the band gap decreases from 1.2 to 0.4 eV. If the mobility and DOS at E_F remain unaffected across $T_{\alpha\beta}$, the conductivity is expected to increase by about nine orders of magnitude, in sharp contrast to the observed three orders of magnitude change. This relatively small change in the conductivity across $T_{\alpha\beta}$, in spite of a large change in the band gap, must be due to the presence of a very low density of states (reduced approximately by about six orders of magnitude) across the gap. Thus it is clear that whatever mechanism responsible for the reduction in the band gap and the consequent change in the electronic conductivity introduces rather low DOS far below the limit of detection of photoemission experiments. However, the results presented here establish that this low DOS is a part of the occupied density of states with E_F continuing to be pinned at the bottom of the conduction band. If the states effectively reducing the band gap occurred below the bottom of the conduction band as a part of the unoccupied DOS, it would necessarily give rise to a substantial shift of E_F (about 0.8 eV) and be easily detected both in the occupied and the unoccupied spectra as a movement of various spectral features relative to the Fermi energy. Moreover, since no new states are being introduced in the system in the case of the $\delta=0$ sample, which also shows the conductivity jump across $T_{\alpha\beta}$, there can only be a redistribution of states from the top of the valence band, leading to the band gap reduction. Obviously this rearrangement near the top of the valence band is intrinsically connected to the disordering of the silver sublattice in the high-temperature phase. Such situations are well known in semiconductor physics where disorder effects are known to lead to an exponential absorption edge, termed the Urbach edge,[19] with a consequent reduction in the band gap. It has been further shown that this arises primarily from an exponential tail at the top of the valence band.[20] While we cannot determine whether the valence band tailing in β-Ag_2S is indeed exponential, the close similarity between these cases may suggest the formation of similar tailing of low DOS from top of the valence band in β-Ag_2S being responsible for the changes in transport properties and the insulator-to-insulator transition observed for Ag_2S across $T_{\alpha\beta}$. However, the present results cannot provide a direct evidence for the formation of such tailing in DOS due to the limits of sensitivity in these experimental techniques and more direct experimental methods may shed more light on the nature of the insulator-insulator transition in Ag_2S in the future.

In conclusion, in this study we have shown that the electronic structure of silver sulfide is well described by one-electron calculations with correlation effects possibly increasing the band gap further. While the XP spectrum is dominated by Ag d-like states, the BI spectrum has major contributions from Ag d- and s-like states. The metal-insulator transition with varying δ in the high-temperature phase is suggested to be due to the tuning of the Fermi energy through the mobility edge. The insulator-to-insulator transition for samples with $\delta\approx0$ across $T_{\alpha\beta}$ is considered to be driven by an order-disorder transition and the consequent tailing of low DOS from the top of the valence band, in close analogy to the formation of Urbach tails in disordered semiconductors.

ACKNOWLEDGMENTS

We thank Professor C. N. R. Rao for his continued support and Dr. R. Cimino for useful discussion. We thank Dr. M. Methfessel, Dr. A. T. Paxton, and Dr. M. van Schiljgaarde for making the LMTO-ASA program available to us and Dr. S. Krishnamurthy for help in setting up the program. We also thank Dr. P. Durham for providing the program to calculate the matrix elements. S.R.B. and N.S. are thankful to the Council of Scientific and Industrial Research, Government of India, for financial support.

*Electronic address: sarma@sscu.iisc.ernet.in

[1] P. Rahlfs, Z. Phys. Chem. Abt. B **31**, 157 (1936).
[2] R. J. Cava, F. Reidinger, and B. J. Wuensch, J. Solid State Chem. **31**, 69 (1980).
[3] C. Wagner, J. Chem. Phys. **21**, 1819 (1953).
[4] R. Sadanaga and S. Sueno, Miner. J. Jpn. **5**, 124 (1967).
[5] P. Junod, H. Hediger, B. Kilchör, and J. Wullschleger, Philos. Mag. **36**, 941 (1977).
[6] H. N. Vasan and A. K. Shukla, Bull. Mater. Sci. **3**, 399 (1981).
[7] A. K. Shukla and H. Schmalzried, Z. Phys. Chem. Neue Folge **118**, 59 (1979).
[8] J. Sohège and K. Funke, Ber. Bunsenges. Phys. Chem. **88**, 657 (1984).
[9] P. W. Anderson, Phys. Rev. **109**, 1492 (1958).
[10] A. K. Shukla, D. D. Sarma, and G. Sankar, Proc. Indian Acad. Sci. (Chem. Sci.) **92**, 43 (1983).
[11] C. Sugiura, M. Kitamura, S. Muramatsu, S. Shoji, S. Kojima, Y. Tada, I. Umezu, and T. Arai, Jpn. J. Appl. Phys. **27**, 1216 (1988).
[12] S. R. Barman, Ph.D. thesis, Indian Institute of Science, Bangalore, India, 1994.
[13] H. N. Vasan, Ph.D. thesis, Indian Institute of Science, Bangalore, India, 1990.
[14] H. Winter, P. J. Durham, and G. M. Stocks, J. Phys. F **14**, 1047 (1984).
[15] S. R. Barman and D. D. Sarma, Phys. Rev. B **51**, 4007 (1995).
[16] D. D. Sarma, N. Shanthi, S. R. Barman, N. Hamada, H. Sawada, and K. Terakura, Phys. Rev. Lett. **75**, 1126 (1995); F. Aryasetiawan and O. Gunnarsson, *ibid*. **74**, 3221 (1995); S. Massida, A. Continenza, M. Posternak, and A. Baldereschi, *ibid.* **74**, 2323 (1995).
[17] D. D. Sarma *et al.*, J. Phys. Condens. Matter **1**, 9131 (1989); W. Speier *et al.*, *ibid*. **1**, 9117 (1989).
[18] N. F. Mott, Philos. Mag. **13**, 989 (1966).
[19] G. D. Cody, T. Tiedje, B. Abeles, B. Brookes and Y. Goldstein, Phys. Rev. Lett. **47**, 1480 (1981).
[20] K. Winer and L. Ley, Phys. Rev. B **36**, 6072 (1987); K. Winer, I. Hirabayashi, and L. Ley, *ibid.* **38**, 7680 (1988).